Scaling and interleaving of subsystem Lyapunov exponents for spatio-temporal systems

R. Carretero-González[a] and S. Ørstavik
Centre for Nonlinear Dynamics and its Applications,[b] *University College, London, Gower Street, London WC1E 6BT, United Kingdom*

J. Huke and D. S. Broomhead
Department of Mathematics, University of Manchester Institute of Science & Technology, Manchester M60 1QD, United Kingdom

J. Stark
Centre for Nonlinear Dynamics and its Applications, University College, London, Gower Street, London WC1E 6BT, United Kingdom

(Received 4 August 1998; accepted for publication 30 December 1998)

The computation of the entire Lyapunov spectrum for extended dynamical systems is a very time consuming task. If the system is in a chaotic spatio-temporal regime it is possible to approximately reconstruct the Lyapunov spectrum from the spectrum of a subsystem by a suitable rescaling in a very cost effective way. We compute the Lyapunov spectrum for the subsystem by truncating the original Jacobian without modifying the original dynamics and thus taking into account only a portion of the information of the entire system. In doing so we notice that the Lyapunov spectra for consecutive subsystem sizes are interleaved and we discuss the possible ways in which this may arise. We also present a new rescaling method, which gives a significantly better fit to the original Lyapunov spectrum. We evaluate the performance of our rescaling method by comparing it to the conventional rescaling (dividing by the relative subsystem volume) for one- and two-dimensional lattices in spatio-temporal chaotic regimes. Finally, we use the new rescaling to approximate quantities derived from the Lyapunov spectrum (largest Lyapunov exponent, Lyapunov dimension, and Kolmogorov–Sinai entropy), finding better convergence as the subsystem size is increased than with conventional rescaling. © *1999 American Institute of Physics.* [S1054-1500(99)00502-9]

Extended dynamical systems serve as a basis for the study and modeling of spatio-temporal behavior in a large class of physical, chemical, and biological systems. Such behavior includes periodic patterns, frozen and traveling interfaces, intermittency, spirals, and synchronization. Often, the complex interaction between time and space gives rise to spatio-temporal chaos. The most common and useful tool for the characterization of chaos is given by the Lyapunov exponents. From the Lyapunov spectrum it is possible to estimate bounds for the effective number of degrees of freedom of the system (i.e., the dimension of the attractor). The computation of the Lyapunov spectrum involves matrix manipulation techniques that soon become prohibitive (in terms of both computing time and memory storage) as the original number of system variables gets large (e.g., a few hundred). In this paper we study the possibility of reconstructing the Lyapunov spectrum of the system by using information from a small subsystem, thereby reducing considerably the computer resources involved in the computations. We propose a new rescaling method leading to better estimates of the Lyapunov spectrum and examine the interlacing properties of Lyapunov spectra for consecutive subsystem sizes. In the process we propose a natural method for constructing the Jacobian of systems on high-dimensional lattices.

I. INTRODUCTION

Spatio-temporal systems give rise to a wide range of interesting phenomena that cannot occur in dynamical systems with only a few degrees of freedom. The most common approach to modeling complex spatio-temporal behavior is through the use of partial differential equations (PDEs). The analysis and even the numerical integration of PDEs is usually quite intricate. Thus, if one desires to study the full range of complex spatio-temporal behavior while conserving a relatively simple dynamical framework, a better approach is to consider discrete spatio-temporal systems. By this we mean a collection of coupled simple low-dimensional dynamical units arranged on a spatial lattice. The coupling is usually (but not always) restricted to a finite neighborhood. An immediate advantage of such systems is their straightforward computational implementation. Another possible advantage is that the local dynamics at each lattice site in the uncoupled limit can be thoroughly analyzed. The knowledge of such local dynamics in the uncoupled limit can help to provide some insight of the complexity of the coupled system.

[a]Electronic mail: R.Carretero@ucl.ac.uk
[b]http://www.ucl.ac.uk/CNDA

In this paper we are particularly interested in the characterization of chaos in such extended dynamical systems. The most basic tool for analyzing a chaotic system is its Lyapunov exponents. The Lyapunov exponents are an important invariant of nonlinear dynamical systems and are closely related to other quantities of interest. Consider a discrete spatio-temporal system with N global state variables, where N is the number of local variables times the spatial volume of the system, for example, $N=\eta L^d$ for a d-dimensional cubic lattice of side L with η local variables in each node. For such an N-dimensional system there exist N Lyapunov exponents corresponding to the rates of expansion and/or contraction of nearby orbits in the tangent space in each dimension. The *Lyapunov spectrum* (LS) is defined as the set $\{\lambda_i\}_{i=1}^N$ of the N Lyapunov exponents arranged in decreasing order. The LS is very useful in the characterization of a chaotic attractor since it gives an estimate of its dimension by means of the *Lyapunov dimension* D_{L} (Kaplan–Yorke conjecture[1,2]) defined as

$$D_{\mathrm{L}}=j+\frac{1}{|\lambda_{j+1}|}\sum_{i=1}^{j}\lambda_i, \tag{1}$$

where j is the largest integer for which $\Sigma_{i=1}^{j}\lambda_i>0$. Another useful invariant that can be derived from the LS is the so called *Kolmogorov–Sinai* (KS) *entropy h* that can be bounded from above by the sum of the positive Lyapunov exponents λ_i^+ and that in many cases can be well approximated by[3]

$$h=\sum \lambda_i^+ . \tag{2}$$

The KS entropy quantifies the mean rate of information production in a system, or alternatively the mean rate of growth of uncertainty in a system subjected to small perturbations.

When dealing with extended dynamical systems, the high number of variables, and even the number of effective degrees of freedom, often leads to severe difficulties because of the large amount of resources (computing time and memory space) required for many computations. Therefore it is useful, and often crucial to develop techniques that derive information about the whole system by analyzing a comparatively small subsystem. For dynamical systems with only a few degrees of freedom the computation of the LS is a straightforward task; however, when the number of degrees of freedom gets large (e.g., a few hundred) it becomes a painstaking process.[4–6] In particular, any algorithm to compute the LS must contain two fundamental procedures; one to multiply by the Jacobian at each time step and the other to perform some kind of re-orthonormalization.[7] The latter is required to prevent the Jacobian matrix progressively getting more ill conditioned, until the largest Lyapunov exponent swamps all the others. Such orthogonalization procedures are based upon the factorization of the Jacobian matrix into a product of an orthogonal matrix Q and an upper triangular matrix R. The two most widespread methods for achieving such orthogonalization are based upon modified Gram–Schmidt (MGS) orthogonalization and the so-called HQR decomposition that uses Householder transformations. The MGS-based methods are widely used because of their quite simple numerical implementation though they are known to introduce small errors due to the fact that the orthogonality of the matrix Q may fail. The HQR-based methods are more difficult to implement but they give a better approximation of the LS[8] since they do not have the problem of losing orthogonality of the matrix Q. The difficulty in using any of these methods for computing the LS of systems with a high number of degrees of freedom N is that they require $\mathcal{O}(N^3)$ operations.[8] The usual naive algorithm for matrix multiplication is also $\mathcal{O}(N^3)$, so that overall computing the full LS is an $\mathcal{O}(N^3)$ process [in principle, matrix multiplication can be done faster than $\mathcal{O}(N^3)$ using specialized techniques, but this hardly seems worth doing under the circumstances]. As an example, the computation of the LS using a HQR method for a logistic coupled map lattice with $N=100$ takes a few hours on a standard workstation. When the system size is an order of magnitude larger (e.g., for two or more spatial dimensions) and/or the convergence of the Lyapunov exponents is rather slow, the task quickly becomes infeasible. Therefore one must rely on other techniques to approximate the LS for large systems.

One such technique to estimate the LS for a large system in a fully spatio-temporal chaotic regime is to consider the LS of a relatively small system with exactly the same dynamical equations. It has been observed in a wide range of spatio-temporal systems that the LS for the small system converges to the spectrum of the whole system under appropriate rescaling. In a number of specialized cases, e.g., turbulent Navier–Stokes flows[9] and hard sphere gases,[10,11] there are rigorous results for this phenomenon. However, it seems difficult to prove its occurrence more generally, and certainly there are many systems where it is observed numerically but no rigorous analysis exists. These include coupled logistic maps,[4] chaotic neural networks,[12] coupled map lattices,[13] reaction-diffusion systems[14,15] (lattice of ODEs), turbulent fluids,[16] the Kuramoto–Sivashinsky model[17] (PDEs) and others.

Such a rescaling approach typically consists of evolving a relatively small N_s-dimensional system under the same equations of motion as the original, large, N-dimensional system and approximating the LS of the latter by rescaling the LS of the former by the ratio of volumes N/N_s. This method relies on the linear increase of Lyapunov dimension D_L and KS entropy with the system size (see above references). A physical interpretation of this phenomenon can be given in terms of the thermodynamic limit of the system. A spatio-temporal system in a fully chaotic regime will possess a typical correlation length ξ such that elements further apart than ξ evolve almost independently from each other. The whole system can then be thought of in some sense as the union of several almost independent subsystems of size ξ. In the limit when these subsystems are completely uncoupled the LS repeats itself in each one of them. If an interaction between the subsystems is introduced, one may expect the overall LS not to be significantly altered. Thus in the limit of a large number of degrees of freedom, a number of Lyapunov exponents per ξ volume may be defined. One expects such an intuitive picture to become more accurate in

the limit of a large number of degrees of freedom and a small correlation length. Nevertheless, considering a small N_s-dimensional system generally fails if its size is too small. This is often due to boundary effects becoming stronger as the system size is decreased and affecting the dynamics.

Another possible way of estimating the LS of the original N-dimensional system also based on the above idea is to consider dynamical information from a small subset of variables of the original system. Thus, instead of using all the N variables of the system to build the Jacobian we take only a subset N_s of these variables and then build the Jacobian for this N_s-dimensional subsystem *without* changing the underlying dynamics of the whole original system. An immediate question that arises when carrying out this task is the choice of boundary conditions of the tangent space for the subset variables since some elements of the subsystem are coupled to elements outside of the subsystem region. This becomes more acute as the coupling range is increased. Different methods may be considered for evaluating the Jacobian of the subsystem at the boundaries. One may, for example, consider periodic boundary conditions for the tangent space (Jacobian) of the subsystem although this seems somehow artificial. Another, more sensible, approach consists of considering no interaction from sites outside of the boundaries in the tangent space. In this manuscript we employ the latter method and consider a pragmatic approach to this issue. We take the dynamics of the original N-dimensional system and truncate its Jacobian to extract a smaller sub-Jacobian whose size is computationally manageable (in terms of the HQR decomposition algorithm). We thus consider the entire $N \times N$ Jacobian by iterating the original system and only then extracting a $N_s \times N_s$ sub-Jacobian by a suitable projection in order to compute the LS for this N_s-dimensional subset of variables. It is easy to numerically implement and perform this procedure since the iteration of the original N-dimensional dynamical system is computationally cheap for discrete systems and the Gram–Schmidt orthogonalization is only applied to the truncated $N_s \times N_s$ sub-Jacobian. Thus we save a factor of $(N/N_s)^3$ operations for the LS computation. In practice it is not necessary to compute the whole Jacobian and then truncate since it is possible to build up the sub-Jacobian directly by dropping the calculation of entries outside of the sub-Jacobian domain. However, maintaining the iteration of the whole original system is crucial.

It is worth stressing that there is an important difference between the Jacobian truncation approach and the usual approach of iterating a smaller system. While for the latter technique the physics at the boundaries is preserved, our approach simply takes into account the neighboring effects through the dynamics itself (remember that we keep the original N-dimensional dynamics untouched). By truncating the Jacobian we destroy the physics at the boundaries. This may lead to problems when we truncate a Jacobian corresponding to a high-dimensional lattice if one is not careful in choosing the ordering of the original Jacobian entries (a detailed analysis is given in Sec. III). However, our approach works remarkably well and its implementation is straightforward. From now on we will use the term subsystem to denote the system corresponding to the truncated Jacobian although we are not really considering a subsystem in the physical sense (since we have the above mentioned boundary subtleties).

Aside from the immediate computational and practical benefits and the possibility of taking a subsystem as small as one dynamical unit without affecting the original dynamics, there is one added advantage to the Jacobian truncation technique from a times-series perspective. In many physical systems even though one is generally interested in global properties, one is only capable of measuring a portion of the dynamical variables (or observables) of the system. Thus reconstructing the overall LS by extracting a Jacobian from a small portion of the original system may be very important. We are currently investigating the possibility of estimating the original LS from a time-series reconstruction of the truncated Jacobian.[18]

When applying our truncating technique and examining more closely the Lyapunov spectra in the fully chaotic regime for several spatio-temporal systems, we found that the Lyapunov exponents of two consecutive subsystem sizes N_s and N_s+1 were interleaved. In other words, the ith Lyapunov exponent for the subsystem N_s lies between the ith and $(i+1)$th Lyapunov exponents of the subsystem N_s+1. The interleaving of the eigenvalues for a single matrix is a well-known fact (Cauchy's interlace theorem) and is common in many areas such as Sturm sequences of polynomials.[19] Unfortunately there appears to be no obvious generalisation which would imply the same fact for subsystem Lyapunov spectra.

This paper is organized as follows. In order to study interleaving we begin by examining the properties of subsystem LS in coupled map lattices in Sec. II. In Sec. II A we investigate the simplest case of homogeneous evolution where we are able to prove rigorously that interleaving and rescaling occur. This example also suggests a different rescaling of the subsystem LS that is superior to that hitherto used in the literature. In Sec. II B we study the interleaving and rescaling properties of the subsystem LS in the fully chaotic regime for a coupled map lattice. Applying the new rescaling obtained from the homogeneous case turns out to lead to a much better fit to the whole LS. In Sec. II C we show that by using this rescaling it is possible to extrapolate the whole LS and extract better estimates for the largest Lyapunov exponent, the Lyapunov dimension, and the KS entropy. In Sec. III we examine the interleaving and rescaling for more complex spatio-temporal systems. We notice that the interleaving is not always exact, but the proportion of Lyapunov exponents that do not interleave is very small. We also present some results for two-dimensional systems and point out that one needs to be careful about the choice of subsystem variables. Finally, in Sec. IV we give a brief recapitulation of the results together with a discussion on the applicability of interleaving and rescaling to more general extended dynamical systems.

II. ONE-DIMENSIONAL COUPLED MAP LATTICES

Coupled map lattices[20,21] (CMLs) are a popular choice for the study of fully developed turbulence and pattern for-

mation. The appeal of CMLs is due on one hand to their computational simplicity and on the other to the fact that they display a wide variety of spatio-temporal phenomena ranging from spatio-temporal periodic states[22,23] and traveling interfaces[24,25] to intermittency[26] and turbulence.[27,28] A CML is a discrete space–time dynamical system with a continuous state space, in contrast to cellular automata where the state space is discrete. Let us denote by x_i^n the state of the ith site at time n, where the integer index i runs from 1 to N. The CML dynamics is defined by

$$x_i^{n+1}=(1-\varepsilon)f(x_i^n)+\sum_{k=-l}^{r}\varepsilon_k f(x_{i+k}^n), \tag{3}$$

where we use periodic boundary conditions, f is a real function, and we ask $\Sigma\varepsilon_k=\varepsilon$ as a conservation law. The general CML (3) couples $l\geqslant 0$ left neighbors and $r\geqslant 0$ right neighbors with coefficients ε_k.

A. Interleaving and rescaling for homogeneous states

In order to gain some insight into interleaving and rescaling behavior of the Lyapunov spectrum in extended dynamical systems let us start with the simplest case of all: homogeneous evolution. We define *homogeneous states* as states of the form $X_n=\{x_i^n\}_{i=1}^N$, where $x_i^n=x^n$ is the same for all i. It is trivial that by setting the initial state of the lattice to a homogeneous state $x_i^0=x^0$ one has that $X_n=\{f^n(x^0)\}$ for all i at any future time n. In other words the homogeneity of the initial state is preserved under iteration by (3).

Let us take a simple form for the coupling by using the most widespread model of a CML, the so-called *diffusive* CML:

$$x_i^{n+1}=(1-\varepsilon)f(x_i^n)+\frac{\varepsilon}{2}(f(x_{i-1}^n)+f(x_{i+1}^n)), \tag{4}$$

where now the coupling is symmetric and only between nearest neighbors. We shall perform a linear stability analysis of homogeneous states in this system. Such an analysis for more general CMLs has also served as the starting point for the study of signal propagation[29] and pattern formation.[22] Since (4) preserves homogeneity under iteration it is natural to ask whether the stability of f completely determines the stability of the homogeneous state. The answer turns out to be yes.

The Lyapunov exponents λ_i are given by the logarithms of the eigenvalues of the matrix

$$\Gamma=\lim_{n\to\infty}[P(n)^{\mathrm{tr}}\cdot P(n)]^{1/2n}, \tag{5}$$

where

$$P(n)=J(n)\cdot J(n-1)\cdots J(2)\cdot J(1),$$

and where $J(s)$ is the Jacobian matrix of the CML dynamics at time s and $(\cdot)^{\mathrm{tr}}$ denotes matrix transpose. The existence of the limit in Eq. (5) for almost every orbit (with respect to an ergodic invariant measure) is guaranteed by the multiplicative ergodic theorem.[30] For the homogeneous lattice

$$J(n)=\mu_n\cdot M \tag{6}$$

where $\mu_n=f'(x^n)$ is the multiplier of the local map and M is the constant matrix

$$M=\begin{pmatrix} 1-\varepsilon & \varepsilon/2 & 0 & \cdots & \varepsilon/2 \\ \varepsilon/2 & 1-\varepsilon & \varepsilon/2 & \cdots & 0 \\ 0 & \varepsilon/2 & 1-\varepsilon & \cdots & 0 \\ \vdots & \ddots & \ddots & \ddots & \vdots \\ \varepsilon/2 & \cdots & 0 & \varepsilon/2 & 1-\varepsilon \end{pmatrix}.$$

The matrix M is not only symmetric but also *circulant*. Recall that a matrix is circulant if in each successive row the elements move to the right one position (with wrap around at the edges).[31] It is straightforward to prove[32] that the eigenvalues of a circulant matrix

$$C=\begin{pmatrix} c_0 & c_1 & \cdots & c_{N-1} \\ c_{N-1} & c_0 & \cdots & c_{N-2} \\ \vdots & \ddots & \ddots & \vdots \\ c_1 & c_2 & \cdots & c_0 \end{pmatrix}$$

are given by $c_0+c_1r_j+\cdots+c_{N-1}r_j^{N-1}$, where $r_j=\exp(2\pi ij/N)$ is an Nth root of unity. Thus, the eigenvalues $\beta_j(n)$ of $J(n)$ are given by

$$\beta_j(n)=\mu_n\left((1-\varepsilon)+\frac{\varepsilon}{2}(r_j+r_j^{N-1})\right)=\mu_n\phi_j(\varepsilon,N),$$

where

$$\phi_j(\varepsilon,N)=(1-\varepsilon)+\varepsilon\cos\left(\frac{2\pi j}{N}\right). \tag{7}$$

It is important to notice that $\phi_j(\varepsilon,N)$ does not depend on the iteration n: the time dependence has been decoupled (factorized) into μ_n. The Lyapunov exponents are then given by

$$\begin{aligned}\lambda_i&=\lim_{t\to\infty}\ln\prod_{n=1}^{t}|\beta_i(n)|^{1/t}\\&=\lim_{t\to\infty}\ln\left(|\phi_i(\varepsilon,N)|\prod_{n=1}^{t}|\mu_n|^{1/t}\right)\\&=\ln|\phi_i(\varepsilon,N)|+\lim_{t\to\infty}\frac{1}{t}\sum_{n=1}^{t}\ln|\mu_n|.\end{aligned}$$

Thus by defining λ_0 to be the Lyapunov exponent of a typical orbit of a single, uncoupled, local map, starting at x^0: $\lambda_0=\lim_{t\to\infty}(1/t)\Sigma_{n=1}^{t}\ln|\mu_n|$, one obtains the following expression for the Lyapunov exponents of a homogeneous evolution:

$$\lambda_i=\lambda_0+\ln|\phi_i(\varepsilon,N)|. \tag{8}$$

Note that the Lyapunov exponents defined by (8) are not arranged in decreasing order. From now on we consider the simple case $\varepsilon<1/2$ so the absolute value inside the logarithm in Eq. (8) can be omitted. For $\varepsilon\geqslant 1/2$ the Lyapunov exponents need further reindexing[33] in order to maintain their decreasing order and a similar construction as bellow is possible. Thus, reindexing the Lyapunov exponents for $\varepsilon<1/2$ yields to

$$\lambda_k=\begin{cases}\lambda_0+\ln(\phi_{k/2}(\varepsilon,N)) & k \text{ even},\\ \lambda_0+\ln(\phi_{(k-1)/2}(\varepsilon,N)) & k \text{ odd},\end{cases} \tag{9}$$

where $k=1$ to N. It is clear that $\lambda_k=\lambda_{k+1}$ when k is even, so most of the exponents occur in degenerate pairs, apart from the largest, and, if N is even, the smallest. The linear stability of a homogeneous orbit is then characterized by the Lyapunov exponent λ_0 of a single site in the uncoupled case $(\varepsilon=0)$. In particular, if the local map is not chaotic, then the homogeneous evolution is not chaotic either since $\lambda_k\leqslant\lambda_0$ $[|\phi_k(\varepsilon,N)|\leqslant 1$ for all $k]$.

It is interesting to notice that the same shape for the LS of a homogeneous CML [cf. (8)] is obtained for a lattice of coupled Bernoulli shifts[33,34] for *any* orbit. There is, however, an important difference: while in the CML the LS dependence on the actual orbit was decoupled thanks to the homogeneity; in the case of coupled Bernoulli shifts, the LS is decoupled from the orbit because the derivative of the local map at any point is constant. Examining further this similarity, if one takes the fully chaotic logistic map $(4x(1-x))$ as the local map for the diffusive CML, the LS for the homogeneous evolution is

$$\lambda_i=\ln 2+\ln(\phi_i(\varepsilon,N)). \tag{10}$$

In fact, any one-dimensional map whose Lyapunov exponent is $\lambda_0=\ln 2$ gives rise to the LS (10) under homogeneous evolution. The LS (10) corresponds exactly to the LS of a lattice of coupled Bernoulli shifts and thus the results described below for the rescaling of the subsystem LS are valid for the case of a lattice of coupled Bernoulli shifts.

According to the discussion in the Introduction, let us perform the LS analysis of the truncated version of the original Jacobian. Thus instead of taking all the sites $i=1,...,N$ to construct the Jacobian we take N_s sites starting at any position j. The choice of j is not important since we are dealing with periodic boundary conditions and because the state is homogeneous; from now on we choose $j=1$. Then we neglect any contribution towards the Jacobian from sites outside of $i\in[1,N_s]$ and consider that the boundary effects come solely from the dynamics itself.[13,15,35] Thus, in our approach, we consider the Jacobian of the subsystem as a principal submatrix J' of size $N_s\times N_s$ from the whole Jacobian J. Here again, once the size of the subsystem is fixed, the particular choice of which principal submatrix to take is not relevant because of the translational symmetry of the system. It is very important to clarify that our approach relies on evolving the dynamics of the whole original system at all times. It is only when one wants the information in tangent space that a principal submatrix of the Jacobian is extracted. By doing so one is including the effects from the neighboring sites through the dynamics itself. The advantages of our approach is that one does not have to deal with the boundary conditions of the subsystem and that the computations are straightforward. This is specially useful when the coupling range is large enough to affect a considerable portion of the sub-Jacobian entries.

The extraction of the principal submatrix J' of the Jacobian J may be written in matrix terms as $J'=\pi(J)$ where π is the following projection

$$\pi(J)=\Pi_l\cdot J\cdot\Pi_r \tag{11}$$

with the left (Π_l) and right (Π_r) projection matrices defined as

$$\Pi_l=(I|Z),$$

$$\Pi_r=\begin{pmatrix}I\\ Z^{\mathrm{tr}}\end{pmatrix},$$

where, from now on, I is the $N_s\times N_s$ identity matrix and Z is the $N_s\times(N-N_s)$ null matrix. Therefore, in order to compute the Lyapunov exponents for the truncated system one has to compute the following product of projected matrices:

$$\begin{aligned}P'(n)&=(\Pi_l J(n)\Pi_r)\cdots(\Pi_l J(2)\Pi_r)(\Pi_l J(1)\Pi_r)\\ &=\Pi_l J(n)\Pi_c J(n-1)\cdots J(2)\Pi_c J(1)\Pi_r,\end{aligned} \tag{12}$$

where

$$\Pi_c=\Pi_r\cdot\Pi_l=\begin{pmatrix}I & Z\\ Z^{\mathrm{tr}} & 0\end{pmatrix}.$$

Multiplying Eq. (12) from the left by the identity matrix obtained by $\Pi_l\cdot\Pi_r=I$ yields

$$\begin{aligned}P'(n)&=\Pi_l\Pi_r\Pi_l J(n)\Pi_c J(n-1)\cdots J(2)\Pi_c J(1)\Pi_r\\ &=\Pi_l\Pi_c J(n)\Pi_c J(n-1)\cdots J(2)\Pi_c J(1)\Pi_r\\ &=\pi(\tilde{P}(n)),\end{aligned} \tag{13}$$

where we define the new product $\tilde{P}(n)=K(n)\cdots K(2)K(1)$ of the projected matrices $K(i)=\Pi_c J(i)$.

Using the above description we obtain the subsystem LS for the homogeneous evolution. The projected Jacobian for the homogeneous evolution at time n is

$$J'(n)=\pi(J(n))=\mu_n\pi(M)=\mu_n\cdot M', \tag{14}$$

where $M'=\pi(M)$ is the $N_s\times N_s$ constant matrix

$$M'=\begin{pmatrix}1-\varepsilon & \varepsilon/2 & 0 & \cdots & 0\\ \varepsilon/2 & 1-\varepsilon & \varepsilon/2 & \cdots & 0\\ 0 & \varepsilon/2 & 1-\varepsilon & \cdots & 0\\ \vdots & \ddots & \ddots & \ddots & \vdots\\ 0 & \cdots & 0 & \varepsilon/2 & 1-\varepsilon\end{pmatrix}$$

if $N_s<N$, and $M'_N=M$ if $N_s=N$. From now on we only use the notation M' when $N_s<N$. It is important to notice that by taking a sub-Jacobian matrix the periodicity at the boundary conditions is lost. Thus, in contrast to M, the matrix M' is not circulant. However, its eigenvalues are well known to be[36]

$$\phi'_j(\varepsilon,N_s)=(1-\varepsilon)+\varepsilon\cos\left(\frac{\pi j}{N_s+1}\right) \tag{15}$$

(where $j=1$ to N_s), and so the eigenvalues $\beta'_j(n)$ of $J'(n)$ are $\beta'_j(n)=\mu_n\phi'_j(\varepsilon,N_s)$. The subsystem LS is given by

$$\lambda'_j=\lambda_0+\ln(\phi'_j(\varepsilon,N_s)). \tag{16}$$

One can immediately infer from this that the Lyapunov exponents for the homogeneous evolution are interleaved for two consecutive subsystem sizes. More precisely, suppose

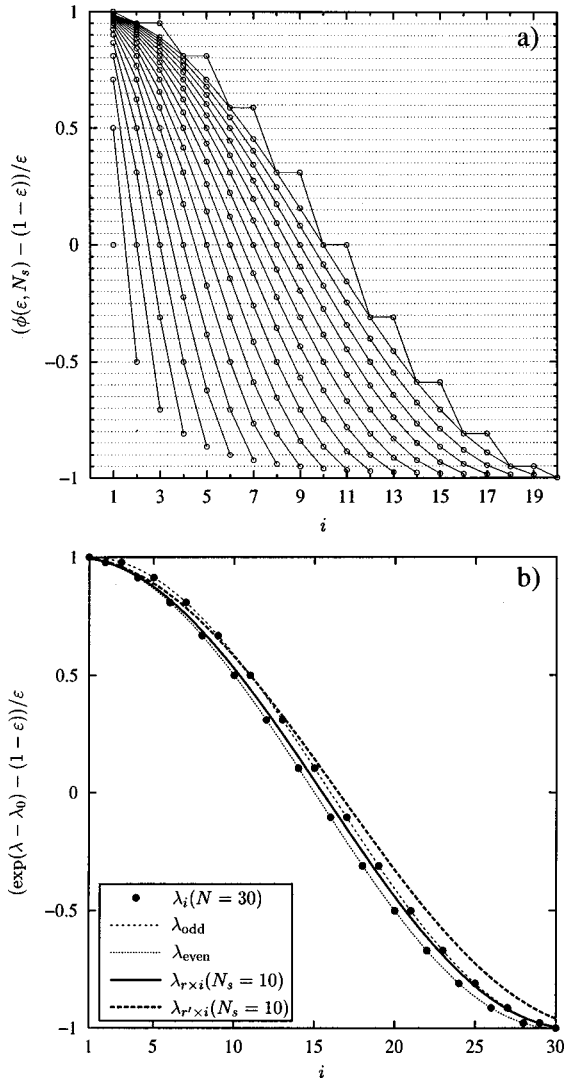

FIG. 1. Lyapunov spectrum for a homogeneous evolution in a diffusive CML: (a) interleaving for subsystem sizes $N_s=1,...,20$ ($N=20$); (b) rescaled subsystem LS, the circles represent the whole LS ($N=30$), the thin dashed lines represent the functions λ_{odd} and λ_{even} passing through the eigenvalues for even and odd indexes, respectively, while the thick lines represent the rescaled LS with $N_s=10$ using the conventional rescaling $r'=N/N_s$ (thick dashed line) and the new rescaling obtained in Sec. II A $r=(N+1)/(N_s+1)$ (thick solid line).

that we take two subsystems, one of size N_s and the other of size N_s+1. It is then trivial to see that their respective Lyapunov exponents $\lambda_i'(N_s)$ and $\lambda_i'(N_s+1)$ satisfy

$$\lambda_i'(N_s+1) \leqslant \lambda_i'(N_s) \leqslant \lambda_{i+1}'(N_s+1) \quad \forall 1 \leqslant i \leqslant N_s, \tag{17}$$

[see Fig. 1(a)]. Interleaving of the subsystem LS with respect to the whole LS $\lambda_i(N)$ also occurs:

$$\lambda_i(N) \leqslant \lambda_i'(N_s) \leqslant \lambda_{i+N-N_s}(N) \quad \forall 1 \leqslant i \leqslant N_s.$$

This interleaving of the eigenvalues is a consequence of Cauchy's interlace theorem[19] that gives bounds on the eigenvalues of a principal submatrix given the eigenvalues of the original matrix. It is important to notice that the interleaving property of the Lyapunov exponents for the homogeneous case is a straightforward consequence of the decoupling of the time dependence of the Jacobian matrix leaving us with the constant matrices M and M'. In a typical nonhomogeneous evolution the time dependence of the Jacobian cannot be factorized and an equivalent constant matrix for the Jacobian does not exist. Therefore, Cauchy's interlace theorem cannot be applied in this general case and there is no reason *a priori* for the interleaving property to hold for a generic extended dynamical system. It is true that, at any particular time, there is interleaving between the eigenvalues of the whole Jacobian and those of a subsystem. However, when computing the LS, one has to compute the product of the Jacobian matrices while for the subsystem LS one uses the product of the sub-Jacobian matrices and therefore the interleaving of the matrix product is no longer assured. The only way, *a priori*, for the interleaving to work would be to take the product of the whole Jacobians *first* and only then extract the sub-Jacobian. The problem with this procedure is that one has to rely again on re-orthonormalization procedures involving the original matrix size N, making the task impossible for large N. Nevertheless, as we shall see in the following section, the interleaving of the subsystem LS does hold to a great extent in the thermodynamic limit.

Another important point to note from Eqs. (15) and (16) is that the LS of the subsystems all have the same shape. The best way to see this is to rescale the indices of the Lyapunov exponents so that they lie in the range $[0,1]$: so instead of plotting λ against j we plot it against $j/(N_s+1)$. Equations (15) and (16) then show that the points always lie on the graph of the function

$$\lambda(z) = \lambda_0 + \ln[(1-\varepsilon) + \varepsilon \cos(\pi z)], \tag{18}$$

irrespective of the value of N_s. This observation suggests another way of looking at the interleaving property. For a given N_s, the z values of the subsystem LS are equally spaced in the interval $[0,1]$; if we increase N_s by 1, the new z values interleave with the old. Since λ is a monotone function the fact that the z values interleave means that the $\lambda(z)$ values interleave also.

To compare the subsystem LS with that of the full system we should similarly rescale the indices for the latter, so now we plot the full system Lyapunov exponents against $j/(N+1)$ instead of j. The points of this spectrum do not lie on the graph of $\lambda(z)$; however, Eq. (9) shows that they do lie on the graphs of the functions

$$\lambda_{\text{even}}(z) = \lambda(z(1+1/N))$$

(for exponents with even indices) and

$$\lambda_{\text{odd}}(z) = \lambda(z(1+1/N) - 1/N)$$

(for exponents with odd indices), where the function $\lambda(z)$ is given by Eq. (18). Since $z(1+1/N) - 1/N < z < z(1+1/N)$ $(0<z<1)$ and $\lambda(z)$ is a decreasing function we see that $\lambda_{\text{even}}(z) < \lambda(z) < \lambda_{\text{odd}}(z)$. Thus λ_{even} and λ_{odd} are bounding curves for λ [see thin dashed lines in Fig. 1(b)] and converge to it as $N \to \infty$; the differences between λ and the other curves are $\mathcal{O}(1/N)$.

The similarities between the shapes of the Lyapunov spectra of the subsystems and of the whole system mean we can use the subsystem LS to estimate the whole LS: to do this we rescale the indices of the subsystem exponents, plot-

ting λ_j against rj where r is a factor chosen so that the rescaled subsystem LS lies as close as possible to the plot of the full system LS. The above discussion shows that if we choose

$$r = \frac{N+1}{N_s+1}, \tag{19}$$

then the rescaled subsystem LS differs from the full system LS by an amount of $\mathcal{O}(1/N)$.

The scaling given by (19) differs from that used conventionally, which is performed by scaling by

$$r' = \frac{N}{N_s}$$

(see Refs. 4, 12, and 13; for rescaling symmetric LS see Ref. 37). It is clear, however, that using r' will give results that differ from those using r by terms of $\mathcal{O}(1/N_s)$, and, since this is larger than $\mathcal{O}(1/N)$, the errors in the exponents will also be $\mathcal{O}(1/N_s)$. This suggests that scaling (19) should give more accurate results than the conventional scaling; this is certainly true in the homogeneous case. As an example Fig. 1(b) shows the original LS for a homogeneous CML with $N=30$ (circles) along with the rescaled LS with $N_s=10$ using the conventional rescaling r' (dashed line) and the new rescaling r obtained above (solid line). It is clear that the new rescaling gives a much better approximation to the original LS.

B. Interleaving and rescaling for coupled logistic maps

As mentioned in the previous section, the interleaving property for the homogeneous evolution relies on the fact that the Jacobian matrices can be factorized into a time-dependent scalar and a *time-independent* matrix [see Eqs. (6) and (14)]. For a nonhomogeneous evolution the Jacobians cannot be factorized in such a way and thus *a priori* one does not expect interleaving to occur. Surprisingly enough, the numerical evidence points towards interleaving of the subsystem LS for almost every Lyapunov exponent in the fully developed chaotic regime. In this section we shall present such evidence for a logistic CML, and discuss why such behavior might be expected to occur. More general systems will be considered in the following section.

We thus consider the diffusive CML (4) with the fully chaotic logistic map $f(x)=4x(1-x)$ and compute its LS for several values of the coupling parameter ε. As with all numerical work in this paper we employ a fast HQR algorithm for the computation of Lyapunov exponents.[8] We then calculate the subsystem LS using principal submatrices J' of size $N_s=1,...,30$ of the Jacobian. In doing so one is not taking into account the dynamics of the neighboring sites next to the boundary and their effects are considered as noise. Thus, the algorithm consists in computing the LS of the sub-Jacobian J' by truncating the actual Jacobian J at each time step and then applying the HQR algorithm. The results are shown in Fig. 2 where we plot the subsystem LS for increasing subsystem size ($N_s=1,...,30$) for three different values of the coupling parameter. In the figure, the filled circles represent the Lyapunov exponents that do not fulfill the interleaving condition. Strikingly, the LS corresponding to $\varepsilon=0.05$ and $\varepsilon=0.45$ [Figs. 2(a) and 2(b)] are very well interleaved, with the exception of a couple of points. On the other hand,

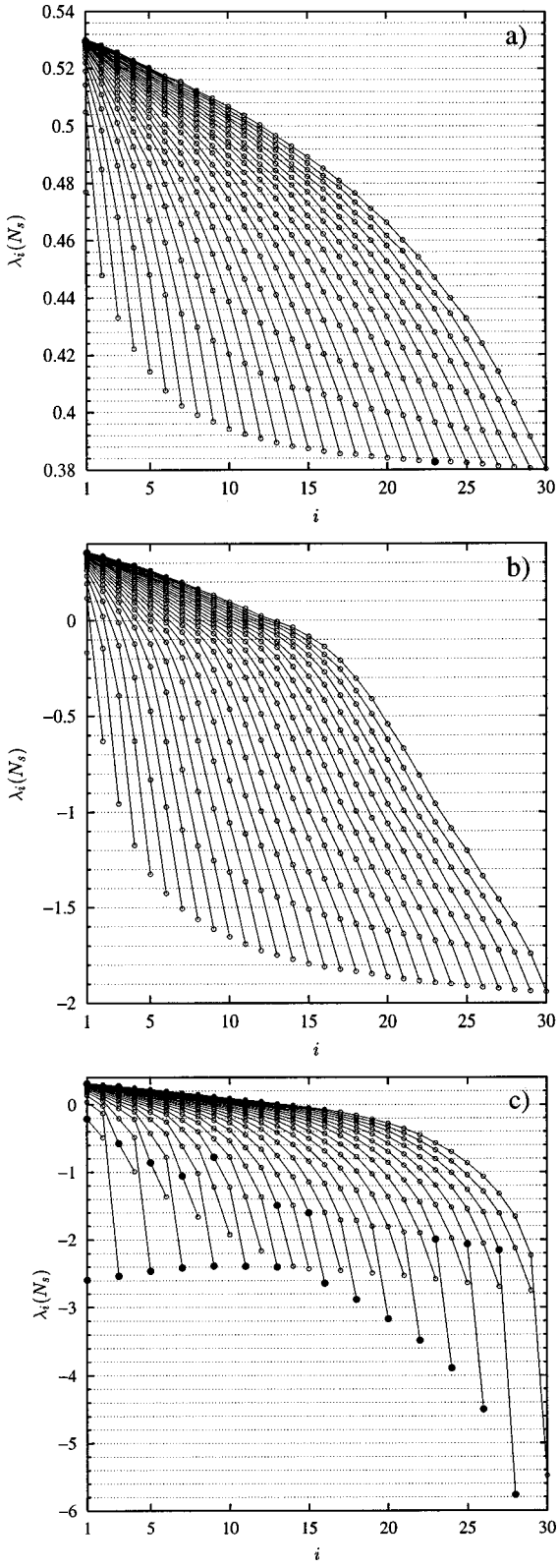

FIG. 2. Subsystem Lyapunov spectra for the fully chaotic coupled logistic lattice $N=100$ for subsystem sizes 1 to 30 (left to right) for (a) $\varepsilon=0.05$, (b) $\varepsilon=0.45$, and (c) $\varepsilon=0.95$. The filled circles represent those Lyapunov exponents which fail to interleave.

for $\varepsilon = 0.95$ [Fig. 2(c)] the LS is not that well interleaved for the smallest Lyapunov exponents, although for the large ones the interleaving is as good as for the previous two figures. The reason for this failure for the smallest Lyapunov exponents is that in the limit $\varepsilon \to 1$ the lattice decouples into two independent sublattices: one for odd i and the other for even i. Thus, when successively increasing the subsystem size, one is including in turn contributions from the even and the odd sublattice. This is reflected in a variation in the smallest Lyapunov exponents every time we increase the subsystem size by one, hence the biperiodic nature of the interleaving failure. In fact, by removing the subsystem LS for odd sizes one ends up with almost perfect interleaving. The exact reasons and conditions for the interleaving of the subsystem LS to happen are not yet understood; however, we believe that they are connected with the convergence of the subsystem LS to the full system LS—a convergence which may be expected in the thermodynamic limit (see below).

As mentioned in the Introduction, it has been observed for some time that under appropriate rescaling the subsystem LS approximates the whole LS. The usual argument for this rescaling behavior makes use of the thermodynamic limit. In the previous section, while studying the interleaving of subsystem LS for the homogeneous case, a new rescaling was suggested [see Eq. (19)]. Let us test this for the case of the fully chaotic coupled logistic lattice. In Fig. 3 we compare, for $\varepsilon = 0.05$ and $\varepsilon = 0.45$, the rescaled subsystem LS using the new rescaling $r = (N+1)/(N_s+1)$ (19) (circles) and the conventional one $r' = N/N_s$ (crosses) to the whole LS (lines) for different subsystem sizes ($N_s = 15,...,25$). As is clear from the figures, the new rescaling r gives a much better fit to the original LS than the conventional rescaling.

Let us explore the idea of rescaling the sub-system LS in the thermodynamic limit a bit further. The correspondence between the rescaled LS and the whole LS in Fig. 3 is astonishingly good. The rescaled spectra lie almost perfectly on top of a decreasing curve, therefore, as with the homogeneous case discussed above, it is not surprising that they are interleaved. In general, if the rescaled Lyapunov spectra of the subsystems converge sufficiently quickly to the whole system LS we expect to have good interleaving of the subsystem Lyapunov spectra. On the other hand, if the rescaled subsystem LS does not approximate the whole system LS well, it is not clear that interleaving will occur. To illustrate this we present the rescaled LS using the new rescaling r for $\varepsilon = 0.95$ in Fig. 4. In this case, the rescaled LS does not give such a good approximation to the whole LS (in particular for the smallest Lyapunov exponents) as seen in the other cases ($\varepsilon = 0.05$ and $\varepsilon = 0.45$). As explained above, this is due to the decoupling of the whole lattice into two sublattices when $\varepsilon \to 1$. Therefore, it appears that the non-interleaving of the smallest Lyapunov exponents in Fig. 2(c) is related to the lack of convergence of the subsystem LS. In general, we suppose that failure to interleave is an indication that the subsystem LS has not converged. Clearly, however, the presence of interleaving is not a sure indication that convergence has occurred; this is illustrated by the two-dimensional logistic lattice discussed below.

We believe that the key point in understanding the interleaving behavior is that although in computing the subsystem LS one is using the product of projected matrices (13), one does not modify the original dynamics in any way. Recall that similar matrices share eigenvalues. Thus a feasible explanation for the occurrence of interleaving is to hypothesize that the product of the projected matrices $P'(n)$ is a projection of a $N \times N$ matrix $\mathcal{Q}(\infty)$ which is similar to the limit as $n \to \infty$ of the original product $P(n)$ of the whole Jacobians. In other words, we conjecture that there exists an invertible $N \times N$ matrix S such that

$$\mathcal{Q}(\infty) = \lim_{n \to \infty} S^{-1} P(n) S, \tag{20}$$

where the product of the projected matrices $P'(n)$ in the limit is obtained by projecting $\mathcal{Q}(\infty)$:

$$P'(\infty) = \pi(\mathcal{Q}(\infty)).$$

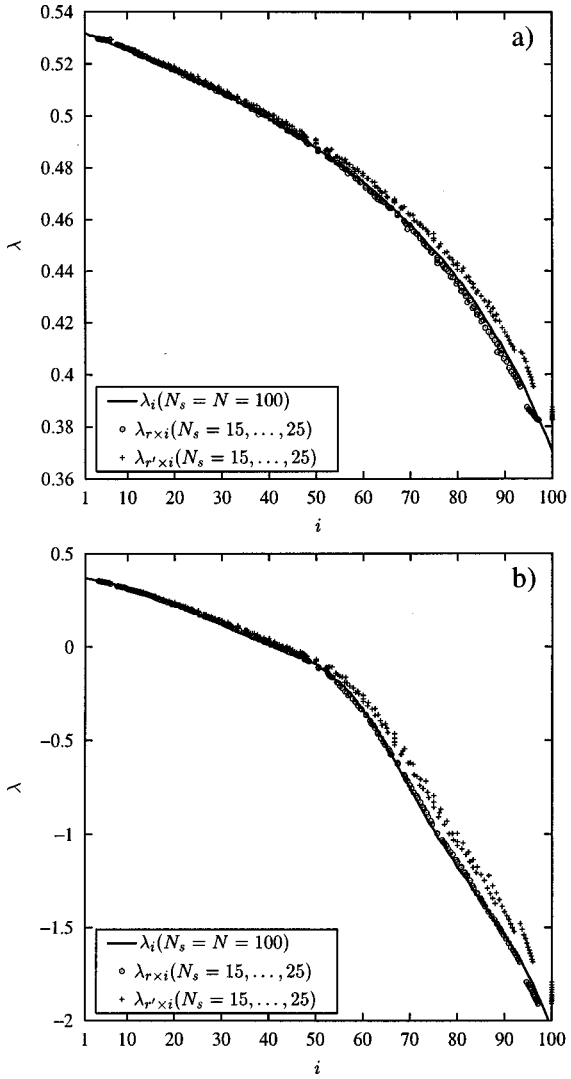

FIG. 3. Comparison of the whole Lyapunov spectrum (solid line) and the rescaled subsystem Lyapunov spectrum using the new rescaling r (circles) and the conventional rescaling r' (crosses) in the fully chaotic logistic lattice with $N = 100$ for several subsystem sizes ($N_s = 15,...,25$): (a) $\varepsilon = 0.05$ and (b) $\varepsilon = 0.45$.

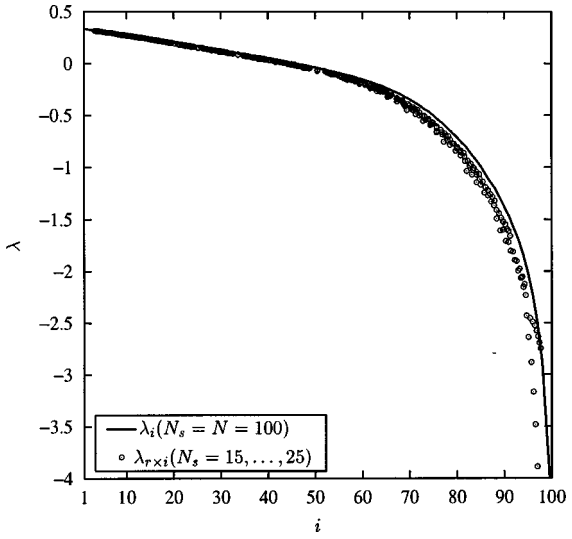

FIG. 4. Rescaled Lyapunov spectrum (circles) for the coupled logistic lattice with $\varepsilon = 0.95$ for subsystem sizes $N_s = 15,...,30$. The solid line represents the whole Lyapunov spectrum $N_s = N = 100$.

Informally, this is saying that in some sense in Eq. (13) the projection matrices commute on average with the Jacobians in the $n \to \infty$ limit. We believe that it might be possible to make this statement rigorous by an appropriate generalization of the multiplicative ergodic theorem.

One might then also ask what is so special about the projection Π_c. Is it possible for interleaving to occur for more general projections? The following two examples suggest that this is indeed the case. Consider the following projection matrices

$$\Pi_1 = \begin{pmatrix} \Pi_1' & Z \\ Z^{\mathrm{tr}} & 0 \end{pmatrix}, \qquad \Pi_2 = \begin{pmatrix} \Pi_2' & Z \\ Z^{\mathrm{tr}} & 0 \end{pmatrix}, \tag{21}$$

where Z is the $N_s \times (N - N_s)$ null matrix and the $N_s \times N_s$ matrices Π_1' and Π_2' are

$$\Pi_1' = \begin{pmatrix} 1 & 1 & 1 & \cdots & 1 \\ 0 & 1 & 1 & \cdots & 1 \\ 0 & 0 & 1 & \cdots & 1 \\ \vdots & \vdots & \vdots & \ddots & \vdots \\ 0 & 0 & 0 & \cdots & 1 \end{pmatrix},$$

$$\Pi_2' = \begin{pmatrix} 1 & \alpha_{12} & \alpha_{13} & \cdots & \alpha_{1N_s} \\ 0 & 1 & \alpha_{23} & \cdots & \alpha_{2N_s} \\ 0 & 0 & 1 & \cdots & \alpha_{3N_s} \\ \vdots & \vdots & \vdots & \ddots & \vdots \\ 0 & 0 & 0 & \cdots & 1 \end{pmatrix},$$

where the α_{ij} are random numbers chosen from the interval $[0, 1]$ with equal probability. Note that we are still using the term projection matrices for Π_1 and Π_2 which in a strict sense is not correct, since they do not satisfy $\Pi_j = \Pi_j^2$ ($j = 1,2$). We use this terminology to stress the fact that they completely remove some of the entries of the original Jacobian. Thus, instead of taking the projection matrix Π_c, let us take Π_1 and Π_2. For the projection Π_2 we randomize its entries *every* time-step; similar results were obtained by randomizing only at the beginning and keeping the same projection matrix thereafter. In Fig. 5 we depict the non-rescaled subsystem LS using both projection matrices for the fully chaotic logistic lattice. The figure strongly suggests that in these cases interleaving still occurs. It thus appears that the choice of projection matrix is not a crucial ingredient for interleaving. Nonetheless, it is important to say that we do not expect interleaving to hold if one uses a series of projection matrices such that when computing the LS one does not get convergence. In the above examples, Π_1 and Π_2, we do have the required convergence. For the Π_2 case, the convergence of the LS of their product is a well-known fact.[38,39]

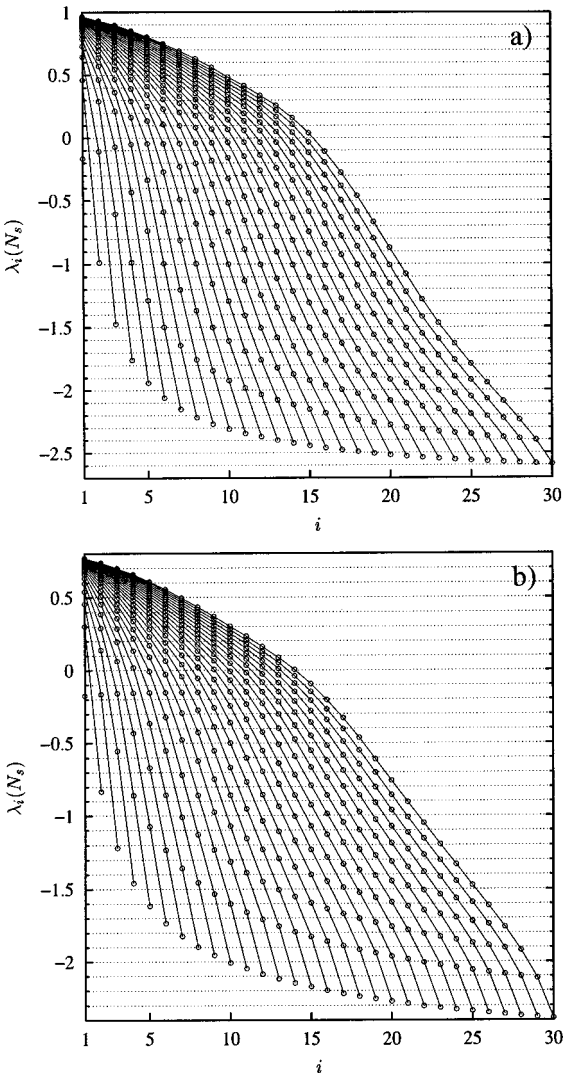

FIG. 5. Interleaving of the subsystem LS, $N_s = 1,...,30$, for the fully chaotic logistic lattice with $\varepsilon = 0.45$ using the more general projection matrices (21) to extract the subsystem Jacobians: (a) Π_1 and (b) Π_2.

On the other hand, when we turn to rescaling we find that although for Π_1 and Π_2 we still get convergence of the rescaled subsystem LS to a definite limit, this limit is not the

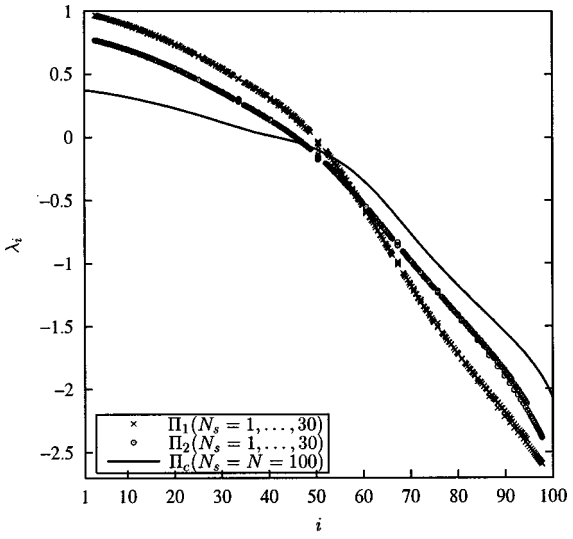

FIG. 6. Rescaled subsystem LS corresponding to Fig. 5 using the projection matrices Π_1 (crosses) and Π_2 (circles). The continuous line corresponds to the original LS computed with the whole Jacobian.

original LS for the full system (Fig. 6). The reason for this discrepancy is easy to understand since the new projections Π_1 and Π_2 combine the entries of the projected Jacobians and thus one expects the eigenvalues to change.

C. Estimation of quantities derived from the Lyapunov spectrum

As illustrated in the previous section, the LS can be well approximated by the rescaled subsystem LS in the thermodynamic limit. We now use the new rescaling in order to approximate the original LS by extrapolating from the subsystem LS. We estimate the largest Lyapunov exponent, Lyapunov dimension, and KS entropy and we compare our method to the results obtained with the whole LS and with the conventional rescaling.

The first method to approximate quantities derived from the LS in the thermodynamic limit is by defining intensive quantities from the extensive ones by simply using the corresponding densities.[5,12,15,35] Let us define the densities of (1) and (2):

$$\rho_d(N_s)=\frac{D_{\mathrm{L}}}{N_s},\qquad \rho_h(N_s)=\frac{h}{N_s}, \tag{22}$$

corresponding to the Lyapunov dimension density and the KS entropy density, respectively. In the thermodynamic limit these densities are intensive quantities (i.e., they do not depend on the subsystem size taken). One then estimates their extensive counterpart when $N_s \to N$ by multiplying the densities (22) by N. To estimate the largest Lyapunov exponent for the whole system we directly take the value of the largest Lyapunov exponent of the subsystem (the Lyapunov exponents are not extensive quantities). It is worth mentioning that in order to use these intensive densities to estimate extensive ones we are supposing the size N of the original system to be known.

The second method, which we believe is more accurate, consists of taking the subsystem LS, rescaling it, extrapolating a curve through it to obtain an approximation to the whole LS, and only then computing the desired quantities. There are several ways to extrapolate the whole LS from the subsystem LS; here we have chosen a piecewise linear approximation for simplicity. One could use more accurate methods such as cubic splines, but the aim here is to compare both kinds of rescaling and thus a piecewise linear fit is the most straightforward approach. Therefore, take the rescaled LS $\lambda_i(N_s)$, obtained with either rescaling for a subsystem of size N_s, and consider the polygon $\mathcal{P}$ through all the points $(i,\lambda_i(N_s))$. To estimate a Lyapunov exponent of the whole LS lying between $\lambda_1(N_s)$ and $\lambda_{N_s}(N_s)$ one simply uses the fit given by the polygon $\mathcal{P}$. For Lyapunov exponents lying to the left (right) of the polygon use linear extrapolation from the first (last) two points of the rescaled LS. Here again one could use more sophisticated extrapolation methods, but for simplicity we restrict ourselves to the linear one. Once the whole LS is estimated using the above method, or a more complicated one, quantities such as the largest Lyapunov exponent $\lambda_1(N)$, the Lyapunov dimension D_{L}, and the KS entropy h are easily extracted.

In Fig. 7 we compare the estimates of (a) the largest Lyapunov exponent $\lambda_1(N)$, (b) the Lyapunov dimension D_{L}, and (c) the KS entropy h obtained from the intensive densities (diamonds) and the piecewise linear fitting for both rescalings (conventional rescaling with crosses and the proposed new one with circles) as the subsystem size increases for the coupled logistic lattice. The actual values of these quantities calculated with the whole LS correspond to the horizontal lines. For the largest Lyapunov exponent, Fig. 7(a); we notice that the estimates are almost identical for both rescalings (crosses and circles). This is due to the fact that both rescalings tend to coincide for small i [see Fig. 1(b)]. The estimate of the largest Lyapunov exponent by just taking the largest Lyapunov exponent of the subsystem (diamonds) shows a slower convergence than the linear fit methods. For the Lyapunov dimension, Fig. 7(b), the method with the slowest convergence corresponds to the conventional rescaling (crosses), while the approximations derived from densities (diamonds) and from a linear fit with the new rescaling (circles) are quite good (note that the new rescaling method does better than the approach using densities). Finally, for the KS entropy, Fig. 7(c), the estimates using the density (diamonds) and the conventional rescaling (crosses) have similar convergence rates while the new rescaling method (circles) does considerably better. The evidence given by this set of plots tends to indicate that the new rescaling method gives better convergence to the quantities derived from the subsystem LS.

III. MORE GENERAL EXTENDED DYNAMICAL SYSTEMS

So far we have only considered interleaving and rescaling in systems in one spatial dimension with nearest neigh-

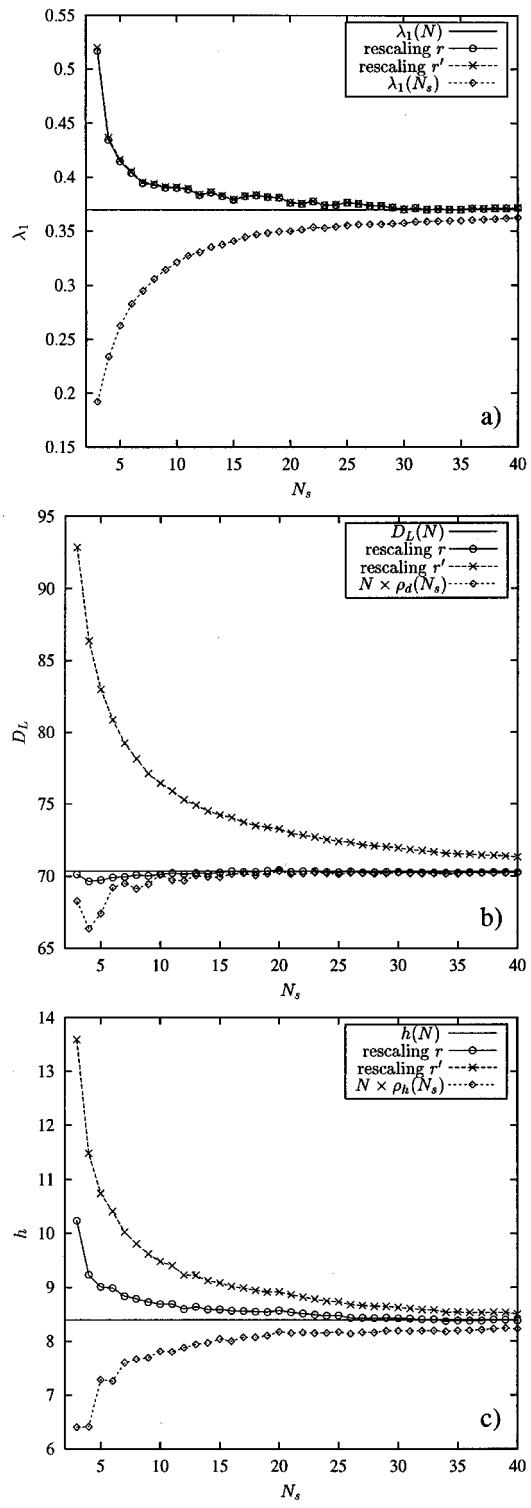

FIG. 7. Estimation of (a) the largest Lyapunov exponent, (b) the Lyapunov dimension and (c) the KS entropy as a function of the subsystem size N_s in the coupled logistic lattice with $N=100$ and $\varepsilon=0.45$. The estimates obtained by using (a) the largest Lyapunov exponent of the sub-system and (b) and (c) the associated densities from the subsystem are presented with diamonds, and the estimate obtained from the piecewise linear fit to the rescaled LS is presented with crosses for the conventional rescaling and circles for the proposed new one. The values obtained with the whole LS are represented by the horizontal line.

bor coupling, corresponding to tridiagonal Jacobians. In this section we turn to more general kinds of extended dynamical systems by allowing a larger coupling range (e.g., chaotic neural networks) and by taking a different topology for the lattice (e.g., lattice with two spatial dimensions). The results presented in this section suggest that the interleaving and rescaling properties observed for the simpler one-dimensional CML persist for more general extended dynamical systems.

A. Chaotic neural networks

We now consider a chaotic neural network[12] of the form

$$x_i^{n+1}=\tanh\left(g\sum_{l=i-k}^{i+k}C_{il}x_l^n\right), \tag{23}$$

where g is a real number called the gain parameter, k represents the connectivity (essentially playing the same role as the range of the coupling in a CML), and the weight matrix C_{ij} has entries chosen randomly from $[-1,1]$ with a uniform probability distribution for $(i-j)(\mathrm{mod}\,N)\leqslant k$ and $C_{ij}=0$ otherwise.

Both the CNN and CML dynamics work in two stages—nonlinearity and coupling—but their order is inverted. The CML dynamics applies the nonlinear mapping f first and then the coupling, while the CNN first applies the coupling via a linear weighted combination of neighboring sites, and then a nonlinear map (the sigmoid). This inversion is reflected in the Jacobian matrix of the transformation: while each entry of the CML Jacobian (6) depends on a single site, each entry of the CNN Jacobian depends on a neighborhood of sites:

$$J_{ij}(n)=\frac{gC_{ij}}{\cosh^2\left[\sum_{l=i-k}^{i+k}C_{il}x_l^n\right]}. \tag{24}$$

The CNN Jacobian (24) inherits the zeros of the coupling matrix C_{ij}, i.e., $J_{ij}(n)=0$ if $(i-j)(\mathrm{mod}\,N)>k$. Another difference between the CNN that we will consider and the diffusive CML discussed before is that the CNN involves coupling with a larger neighborhood than just the left and right nearest-neighbors.

Let us now analyze the interleaving and rescaling for a CNN with a large k. In Fig. 8 we show the interleaving and rescaling with $k=10$ and $g=2$. As we can see, the interleaving is quite good with the exception of a few small Lyapunov exponents. In Fig. 8(b) we plot the rescaled subsystem LS for several subsystem sizes using both rescalings (circles: new rescaling and crosses: conventional rescaling) along with the whole LS (solid line). Clearly the new rescaling gives a better estimate of the whole LS. Similar results were obtained for other values of the parameters k and g.

B. Two-dimensional logistic lattice

The interleaving and rescaling properties of the subsystem LS were obtained in Sec. II A for a one-dimensional array of coupled maps. Here we put to the test the interleaving and rescaling for a two-dimensional CML. Let us take a

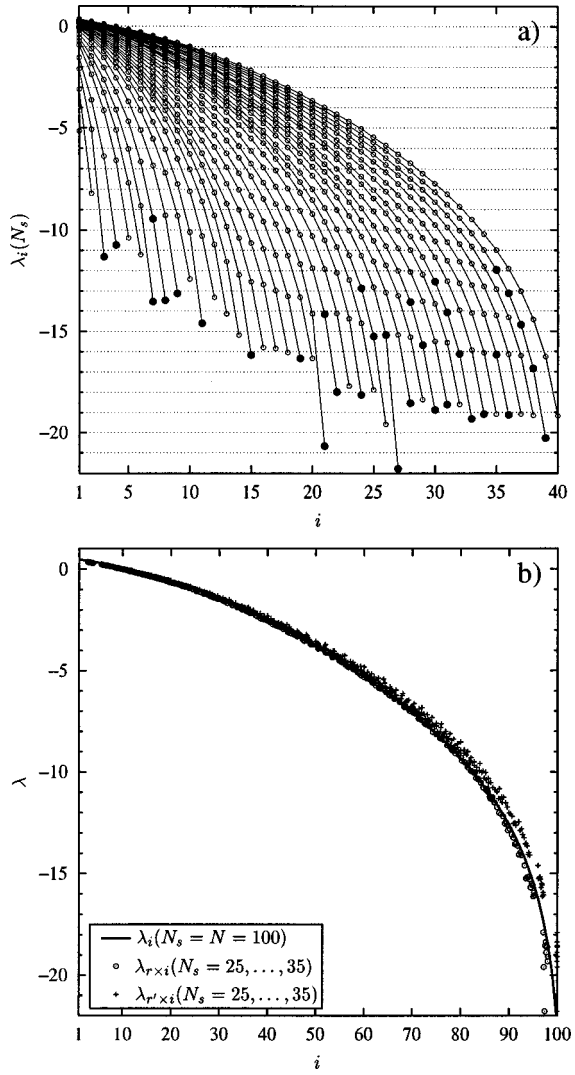

FIG. 8. (a) Interleaving of the subsystem LS in the chaotic neural network (23) with $k=10$ and $g=2$. (b) Comparison between the conventional rescaling of the subsystem Lyapunov spectrum (crosses) and the new rescaling obtained in Sec. II A (circles); the whole LS is depicted by the solid line.

two-dimensional square lattice of size $L\times L$. The local dynamics x_{ij}^n at each node (i,j) and any time n is governed by the fully chaotic logistic map

$$f_{ij}(x)=f(x)=4x(1-x).$$

As in the one-dimensional CML the local dynamics is applied first,

$$y_{ij}^n(x)=f(x_{ij}^n),$$

and then the coupling dynamics

$$x_{ij}^{n+1}=(1-\varepsilon)y_{ij}^n+\varepsilon\overline{y}_{\mathcal{N}_{ij}}^n,$$

where $\overline{y}_{\mathcal{N}_{ij}}^n$ is the average of the y_{ij}^n in the neighborhood $\mathcal{N}_{ij}$ of site (i,j). The neighborhood $\mathcal{N}_{ij}$ is taken to be the eight adjacent sites to (i,j) with periodic boundary conditions.

The Jacobian $J(n)$ at time n for this two-dimensional lattice is defined through its elements:

$$J_{kl}(n)=\frac{\partial x_{\sigma_k}^{n+1}}{\partial x_{\sigma_l}^n},$$

where the indices σ_k and σ_l refer to the position in the actual lattice of the chosen kth and lth state variables of the system. If one just wants to compute eigenvalues of the whole Jacobian, the order in which the state variables are taken is not relevant. However, we are interested in extracting sub-Jacobian matrices from the whole system and thus the ordering choice of the state variables does matter. There are $L^2!$ different ways to choose the ordering, but the simplest way consists of taking the site (1,1) as the first state variable and then proceeding horizontally to the right until the end of the lattice is reached and then proceeding to the bottom of the lattice by rows:

1	2	3	$\ldots$	$L-1$	L
$L+1$	$L+2$	$L+3$	$\ldots$	$2L-1$	$2L$
$2L+1$	$2L+2$	$2L+3$	$\ldots$	$3L-1$	$3L$
$\vdots$	$\vdots$	$\vdots$		$\vdots$	$\vdots$

,

that is $\sigma_k=(k-\lfloor k/L\rfloor,\lfloor k/L\rfloor)$ where $\lfloor z\rfloor$ denotes the largest integer smaller than or equal to z. From now on this kind of ordering will be called *horizontal wraparound*. There is obviously a vertical counterpart where the order is taken by columns. The problem with this type of ordering is that it does not build up the Jacobian in a natural way. The propagation of a perturbation typically grows equally in both of the two spatial dimensions (in particular for our choice of coupling since all the neighbors contribute with the same weight $\varepsilon/8$). In contrast, with horizontal or vertical wraparound one has to wait until a complete wrap is taken to fall again near the perturbed area. A more natural approach might thus be to attempt to mimic the spatial growth of perturbations by taking an ordering that fills up a two-dimensional area from the centre outwards. For that purpose, we use the following ordering technique:

1	2	5	10	$\cdots$
4	3	6	11	$\cdots$
9	8	7	12	$\cdots$
16	15	14	13	$\cdots$
$\vdots$	$\vdots$	$\vdots$	$\vdots$	$\ddots$

.

We call this *square wraparound*.

In Fig. 9 we show the non-rescaled subsystem LS for the two wraparound methods, (a) square and (b) horizontal, and we plot with solid circles the Lyapunov exponents that fail to interleave. Observe that interleaving failure occurs for only a very few Lyapunov exponents. After a careful examination of these Lyapunov exponents one notices that they are very close to interleaving, suggesting that the failure is due to numerical error in the computation of the exponents (and in particular poor convergence). Therefore, we shall consider a Lyapunov exponent to be interleaved if it falls in the interval

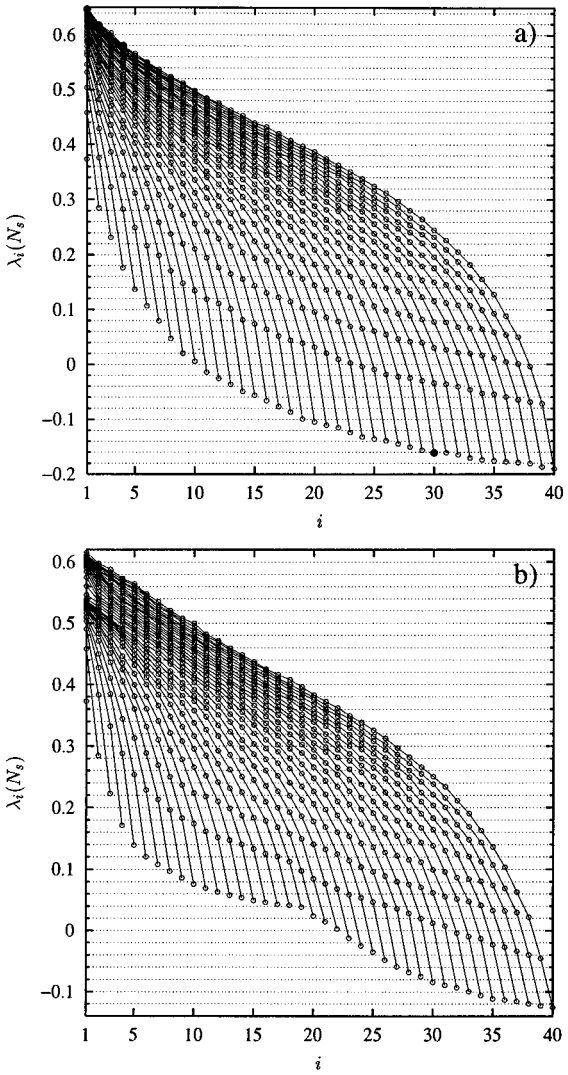

FIG. 9. Subsystem Lyapunov spectra for the two-dimensional 20×20 coupled logistic lattice for subsystem sizes 1 to 40 (left to right) for $\varepsilon=0.45$ and for the two wraparound methods for building up the Jacobian: (a) square wraparound and (b) horizontal wraparound. The filled circles represent the Lyapunov exponents where interleaving fails.

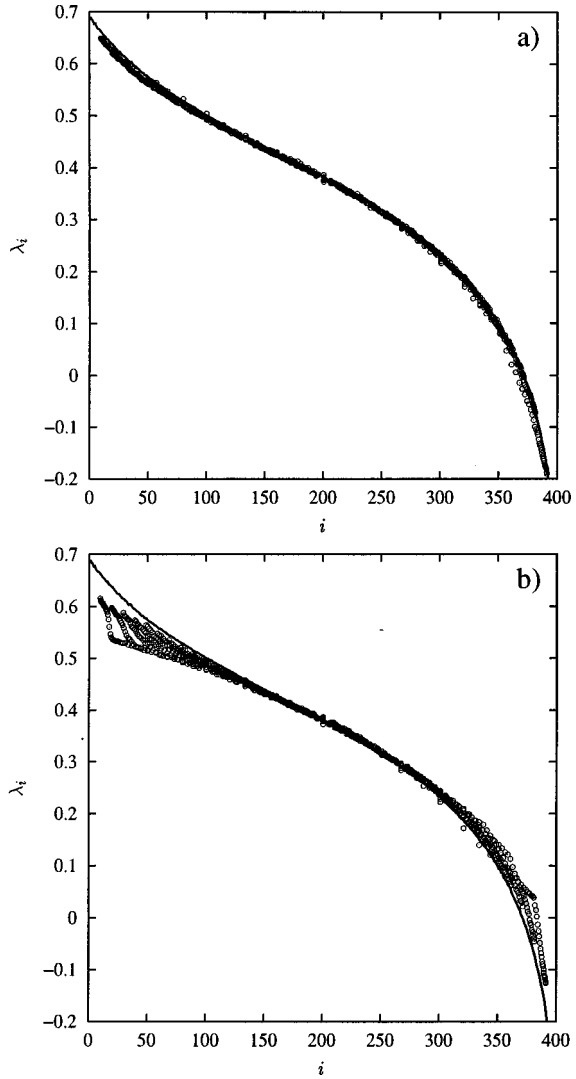

FIG. 10. Rescaled subsystem LS for the two-dimensional coupled logistic lattice (same parameters as in Fig. 9) using (a) square and (b) horizontal wraparound methods.

defined by the inequality (17) with an error δ:

$$\lambda_i(N_s+1)-\delta\Lambda\leqslant\lambda_i(N_s)\leqslant\lambda_{i+1}(N_s+1)+\delta\Lambda, \qquad (25)$$

where $\Lambda=\lambda_{i+1}(N_s+1)-\lambda_i(N_s+1)$. From now on we redefine δ such that the errors are given in percentages. Using such a definition, if one allows a small error of 2.5%—$\delta=0.025$ in (25)—for the Lyapunov exponents in Fig. 9, one obtains perfect interleaving for the whole spectrum.

The interleaving seen in Fig. 9 suggests that the ordering choice for the Jacobian entries does not play an important role in this phenomenon. However, as can be seen in Fig. 10, where we plot the rescaled LS for both wraparound methods along with the whole LS, the choice of ordering method is crucial in obtaining good rescaling behavior. Square wraparound [Fig. 10(a)] yields immediate convergence towards the whole LS: even for a very small subsystem size the rescaled LS is almost exactly superimposed on top of the whole LS. On the other hand, horizontal wraparound [Fig. 10(b)] gives a rescaled subsystem LS that seems to converge to a different curve for subsystem sizes $N_s=1,...,20$ (aligned points in the lower part of the curve for the first Lyapunov exponents). For subsystem sizes larger than 20, the rescaled LS starts a new convergence towards something closer to the whole LS. The explanation for this phenomenon is quite simple. The Jacobian for the horizontal wraparound consists of a main diagonal of nonzero elements coming from the neighbors in the same row of the square lattice; however, the neighbors in the row above and below give rise to two subdiagonals of nonzero elements. The subdiagonals start when a whole wraparound has been completed, that is, when $N_s=L$ where L is the side length of the square lattice. Thus for subsystem sizes $N_s<L$, the sub-Jacobian only extracts the main diagonal elements and does not capture the two subdiagonals with vital information about the neighboring sites in the rows above and below. When $N_s\geqslant L$, the sub-Jacobian starts capturing these forgotten neighbors and the rescaled subsystem LS now begins to converge to the desired LS. For example, in Fig. 10(b) this behavior starts at $N_s=L=20$.

In order to illustrate the effects of the horizontal wrap-

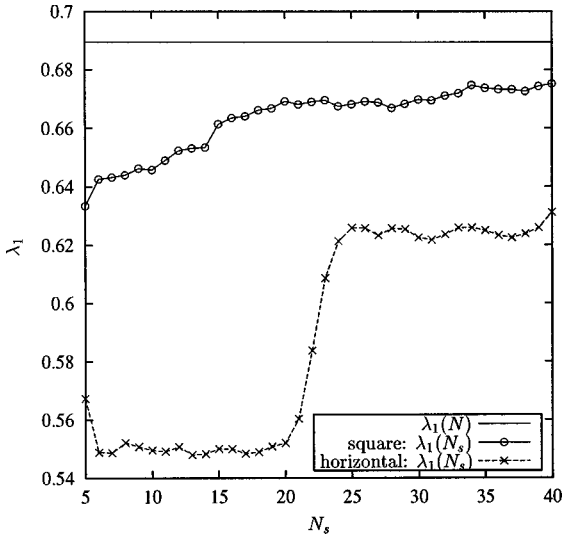

FIG. 11. Estimation of the largest Lyapunov exponent as a function of the subsystem size N_s in a two-dimensional logistic lattice of size 20×20 and with $\varepsilon=0.45$ using a linear fit for the rescaled subsystem LS. The circles correspond to building up the Jacobian by square wraparound while the crosses correspond to horizontal wraparound. The value of the largest Lyapunov exponent for the whole lattice is represented by the horizontal solid line.

around we depict in Fig. 11 an estimate of the largest Lyapunov exponent by extrapolating the whole LS from its rescaled version as the subsystem size increases. The results are depicted with circles for square wraparound and with crosses for horizontal wraparound. The vertical solid line corresponds to the largest Lyapunov exponent from the whole LS. The estimate using horizontal wraparound seems to converge to a much smaller value than the desired one for subsystem sizes $N_s<L=20$. When the subsystem size is increased further, horizontal wraparound performs better but still lacks the desired convergence. On the other hand, the square wraparound converges rapidly in a smooth way: this is because it was designed to build up the Jacobian entries in a more natural way. Therefore, although the interleaving for both wraparound methods is very good, it is not advisable to use the horizontal wraparound. Moreover, in the thermodynamic limit $L\to\infty$, the method of the horizontal wraparound completely fails since it is unable to effectively wrap, even for very large subsystem size, and thus the important contribution of a large part of the neighbors (six out of eight for two-dimensional lattices and worse for higher-dimensional lattices) is not reflected in the sub-Jacobian. In this limit the plateaus observed in Fig. 11 for the horizontal wraparound would become infinitely large and thus one cannot expect to estimate accurately any quantity derived from the Lyapunov spectrum.

C. Host–parasitoid system

We now consider a more general type of two-dimensional lattice, namely the Host–parasitoid lattice model.[40–42] For this system the local dynamics is no longer one-dimensional but two-dimensional: hosts and parasites. The model evolves again in two phases. First there is at each site (i,j) a local dynamics given by

$$\begin{aligned}\mathcal{H}_{ij}^n &= bH_{ij}^n e^{-aP_{ij}^n},\\ \mathcal{P}_{ij}^n &= cH_{ij}^n(1-e^{-aP_{ij}^n}),\end{aligned} \tag{26}$$

where H^n and P^n are, respectively, the population size of hosts and parasitoids at time n,a is the per capita parasitoid attack rate, b is the host reproductive rate, and c is the conversion efficiency of parasitized hosts into female parasitoids in the next generation. The second phase involves dispersal into a neighborhood $\mathcal{N}_{ij}$ of site (i,j), i.e., a fraction μ_h of hosts and μ_p of parasitoids disperse equally into the eight neighboring sites:

$$\begin{aligned}H_{ij}^{n+1} &= (1-\mu_h)\mathcal{H}_{ij}^n+\mu_h\overline{\mathcal{H}}_{\mathcal{N}_{ij}}^n,\\ P_{ij}^{n+1} &= (1-\mu_p)\mathcal{H}_{ij}^n+\mu_p\overline{\mathcal{P}}_{\mathcal{N}_{iij}}^n,\end{aligned} \tag{27}$$

where $\overline{\mathcal{H}}_{\mathcal{N}_{ij}}^n$ and $\overline{\mathcal{P}}_{\mathcal{N}_{ij}}^n$ are, respectively, the average of the hosts and the parasitoids [after local dynamics (26)] in the neighborhood $\mathcal{N}_{ij}$ of site (i,j). We take a square lattice $(i,j)\in[1,L]^2$ and periodic boundary conditions. The total size of the system is then $N=2L^2$. Let us build up the whole Jacobian with host–parasite blocks of size 2×2:

$$J=\begin{pmatrix} \mathcal{J}_{\sigma_1}^{\sigma_1} & \mathcal{J}_{\sigma_2}^{\sigma_1} & \cdots & \mathcal{J}_{\sigma_{L^2}}^{\sigma_1}\\ \mathcal{J}_{\sigma_1}^{\sigma_2} & \mathcal{J}_{\sigma_2}^{\sigma_2} & \cdots & \mathcal{J}_{\sigma_{L^2}}^{\sigma_2}\\ \vdots & \vdots & \ddots & \vdots\\ \mathcal{J}_{\sigma_1}^{\sigma_{L^2}} & \mathcal{J}_{\sigma_2}^{\sigma_{L^2}} & \cdots & \mathcal{J}_{\sigma_{L^2}}^{\sigma_{L^2}}\end{pmatrix},$$

where the host–parasite blocks $\mathcal{J}_{\sigma_j}^{\sigma_i}$ are given by

$$\mathcal{J}_{\sigma_j}^{\sigma_i}=\begin{pmatrix} \dfrac{\partial H_{\sigma_i}^{n+1}}{\partial H_{\sigma_j}^n} & \dfrac{\partial H_{\sigma_i}^{n+1}}{\partial P_{\sigma_j}^n}\\ \dfrac{\partial P_{\sigma_i}^{n+1}}{\partial H_{\sigma_j}^n} & \dfrac{\partial P_{\sigma_i}^{n+1}}{\partial P_{\sigma_j}^n}\end{pmatrix}.$$

The indices $\sigma_{1,\ldots,L^2}$ refer to the actual position in the two-dimensional lattice of a particular local population. As for the two-dimensional CML, the ordering choice of the Jacobian entries plays an important role for the rescaling.

Given a reasonable lattice size ($L>15$) and depending on the dispersal parameters μ_h and μ_p the evolution of model (27) is spatio-temporally chaotic.[43] Here we choose $L=20$, $a=1$, $b=2$, $c=1$, $\mu_h=0.2$, and $\mu_p=0.6$. The full system is thus $N=2L^2=800$ dimensional. We start the system with random initial conditions and discard a transient of 10^5 iterations before computing the subsystem LS. In Fig. 12 we depict the interleaving of the subsystem LS for subsystem sizes $N_s=1,\ldots,40$ where we allow a 5% error in the interleaving—$\delta=0.05$ in (25). Figures 12(a) and 12(b) correspond to square wraparound while Figs. 12(c) and 12(d) correspond to horizontal wraparound. As the future shows, interleaving is quite good even for the upper region [see amplifications in Figs. 12(b) and 12(d)] where the density of Lyapunov exponents is very high and the intervals for interleaving are small and thus the margin for error in the inequality (25) is reduced. Square wraparound does better for

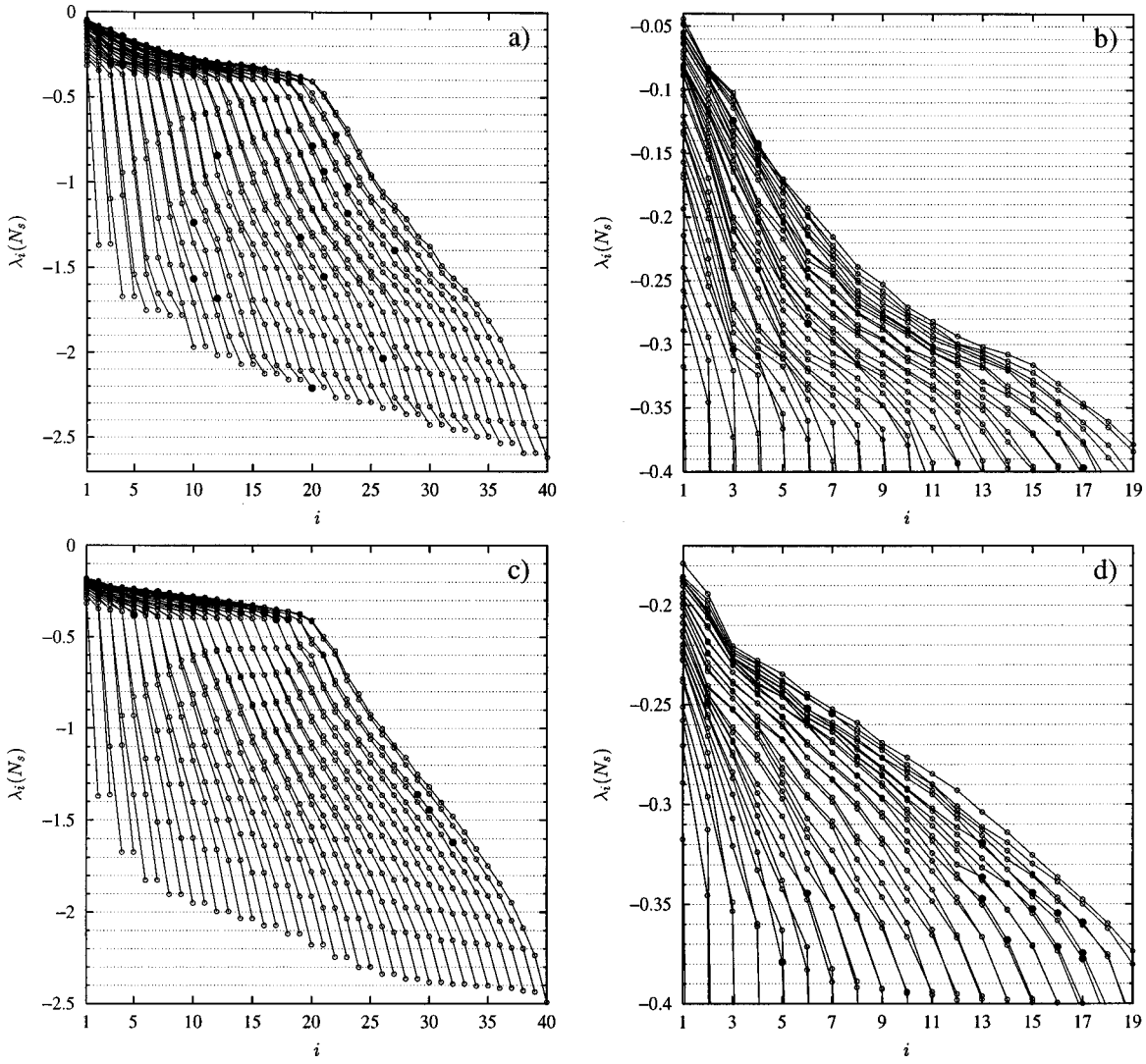

FIG. 12. Interleaving of the subsystem LS for the host-parasite system in a two-dimensional lattice of size 20×20. The Jacobian was built using (a) and (b) square wraparound and (c) and (d) horizontal wraparound. Figures (b) and (d) correspond, respectively, to amplifications of figures (a) and (c) for the top half of the spectrum.

large Lyapunov exponents [Fig. 12(b)] while horizontal wraparound does better for small ones. However, overall both methods have approximately similar performance.

While the choice of wraparound method is not crucial for interleaving, Fig. 13(a) shows that it leads to significant differences in rescaling behavior. Note that the LS for the whole system $N_s=N=800$ is not depicted since it would take an enormous amount of time to compute. In Fig. 13(a) we depict the rescaled LS for subsystem sizes $N_s=1,...,40$ for both wraparound methods (square wraparound with circles and horizontal wraparound with crosses). As for the two-dimensional lattice of coupled logistic maps, horizontal wraparound converges to a different curve than does square wraparound. The reason is again that for the horizontal wraparound one has to wait until a complete wrap is finished until falling again into the neighboring region. In this case, a horizontal wrap of the Jacobian is achieved when $N_s=2L=40$. Moreover, for $N_s=2L=40$ one is only including partial derivatives of hosts with respect to hosts and parasitoids. In order to include dependences of parasitoids with respect to hosts and parasitoids one should take a further wrap of the Jacobian, i.e., $N_s=4L=80$.

Therefore, the horizontal wraparound technique for subsystem sizes $N_s\leqslant40$ does not pick up the dynamics of the neighbors situated in adjacent rows. This problem for horizontal wraparound becomes worse as the dimension of the local dynamics is increased. A partial solution to this problem is to build up the Jacobian by using just one of the local variables of the system. Particularly in the host–parasite system where the parasitoid dynamics is slaved to the host dynamics, one should be able to reproduce the LS from only the host variables. We then build up the Jacobian by taking only host variables using both wraparound methods. The results are shown in Fig. 13(b) where again the circles correspond to square wraparound and the crosses to horizontal wraparound. We only plot the first half of the spectrum; the second half of the spectrum differs considerably for both methods (host–parasites variables and only host variables) since the small Lyapunov exponents are more sensitive to the loss of information contained in the parasite variables. On

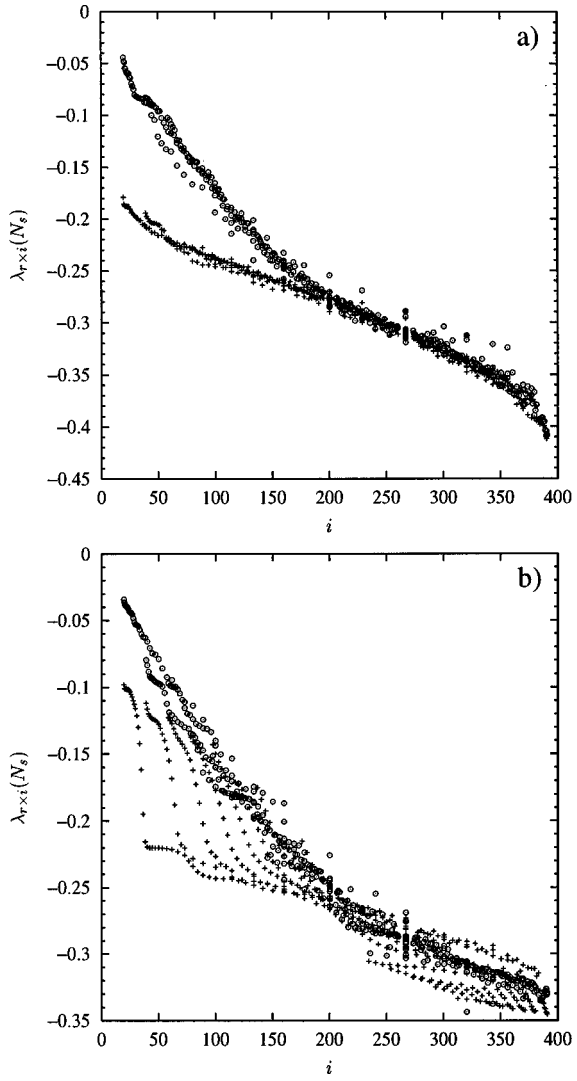

FIG. 13. First half of the rescaled Lyapunov spectrum for a host-parasitoid system in a two-dimensional lattice for subsystem sizes $N_s=1,...,40$. (a) Using both the host and parasite variables and (b) using only the hosts when building up the Jacobian. The circles (crosses) correspond to the square (horizontal) wraparound.

the other hand, the first half of the spectrum is quite similar independently of the choice of host–parasite or only host variables. As we can see in Fig. 13(b), horizontal wraparound seems to converge to a different curve than square wraparound for subsystem sizes $N_s<20$ (see aligned crosses in the lower part of the spectrum). Since we are only taking the host population (20×20), when $N_s>20$ the horizontal wraparound has finished a complete wrap and it starts to pick up the neighbors in adjacent rows and thus the rescaled spectrum begins to converge closer to the square wraparound.

IV. CONCLUSIONS

When studying high-dimensional extended dynamical systems in a spatio-temporal chaotic regime it is possible to rescale the subsystem Lyapunov spectrum to obtain the original Lyapunov spectrum. In this thermodynamic limit, a subsystem of comparatively small size N_s contains a sufficient amount of information to reconstruct the Lyapunov spectrum of the whole system. Usually, when coupling different subsystems in a lattice one chooses a coupling with a finite neighborhood (localized coupling) or at least with decreasing effect for further away neighbors. In the context of discrete spatio-temporal systems, this restriction on the choice of coupling causes the Jacobian of the dynamics to be a banded (or quasi-banded) matrix. In the limit of only nearest neighbors interaction in a one-dimensional lattice, the Jacobian is a tridiagonal matrix. If one considers the homogeneous evolution under this dynamical system, the Lyapunov spectrum of sub-Jacobian matrices will inherit the rescaling and interleaving properties described in Sec. II A. The evidence presented in this paper shows that the new rescaling method of the subsystem Lyapunov spectrum gives a much better fit than the conventional rescaling N/N_s for one-dimensional lattices.

We have also observed interleaving of the Lyapunov spectra for consecutive subsystem sizes. We showed that for two-dimensional lattices the rescaling and interleaving are still valid. However, the choice of variables used to build up the sub-Jacobian matrices appears to be crucial to achieve good rescaling properties. In particular one has to choose an ordering method of the system variables that mimics the propagation of information in the particular lattice topology of the system. In two dimensions we showed that choosing the system variables in ''concentric'' subsquares gave a much better rescaled Lyapunov spectrum than by choosing them in a row or columnwise fashion. Generalizing this idea to higher-dimensional lattices one should take the system variables by filling up ''concentric'' hyper-cubes.

Another point to take into account when choosing the system variables in high-dimensional lattices is the anisotropy of the coupling. The two-dimensional systems studied here have an equal relative contribution from all the neighboring directions (isotropic coupling). It is possible to choose the coupling in order to give more weight to one of the directions (vertical or horizontal) and thus the propagation of information to be faster in that direction. Therefore, instead of building the system variables by ''concentric'' squares, it should be more natural to take rectangles, the ratio of the rectangle sides being related to the ratio of velocity propagation of disturbances in both directions.

For a continuous spatio-temporal system a similar reconstruction may be used by sampling in a grid of a subsystem at regular time intervals and by reconstructing the Jacobian from time series in the usual manner. The same procedure can be applied for a discrete spatio-temporal system where the dynamics is not explicitly given and the only available dynamic information comes from time series taken at several spatial locations. We expect that rescaling and interleaving should still be observed in these cases. This aspect is currently under investigation and will be reported elsewhere.[18]

ACKNOWLEDGMENTS

This work was carried out under EPSRC Grant No. GR/L42513. J.S. would also like to thank the Leverhume Trust for financial support under a Royal Society Leverhume Trust Senior Research Fellowship.

[1] J. L. Kaplan and J. A. Yorke, *Chaotic behaviour of multidimensional difference equations*, Lecture Notes in Mathematics (Springer, New York, 1979) Vol. 730, pp. 204–227.
[2] H. G. Schuster, *Deterministic chaos* (VCH Verlagsgesellschaft, Weinheim, 1988), 2nd ed.
[3] J.-P. Eckmann and D. Ruelle, ''Ergodic theory of chaos and strange attractors,'' Rev. Mod. Phys. **57(3)**, 617–656 (1985).
[4] P. Grassberger, ''Information content and predictability of lumped and distributed dynamical systems,'' Phys. Scr. **40**, 346–353 (1989).
[5] G. P. Puccioni, A. Torcini, A. Politi, and G. D'Alessandro, ''Fractal dimension of spatially extended systems,'' Physica D **53**, 85–101 (1991).
[6] M. Bauer, H. Heng, and W. Martienssen, ''Characterization of spatiotemporal chaos from time series,'' Phys. Rev. Lett. **71(4)**, 521–524 (1993).
[7] K. Geist, U. Parlitz, and W. Lauterborn, ''Comparison of different methods for computing Lyapunov exponents,'' Prog. Theor. Phys. **83(5)**, 875–893 (1990).
[8] H. F. von Bremen, F. E. Udwadia, and W. Proskurowski, ''An efficient QR based method for the computation of Lyapunov exponents,'' Physica D **101**, 1–16 (1997).
[9] D. Ruelle, ''Large volume limit distribution of characteristic exponents in turbulence,'' Commun. Math. Phys. **87**, 287–302 (1982).
[10] Ya. G. Sinai, ''A remark concerning the thermodynamic limit of the Lyapunov spectrum,'' Int. J. Bifurcation Chaos Appl. Sci. Eng. **6(6)**, 1137–1142 (1996).
[11] Ya. G. Sinai and N. I. Chernov, ''Entropy of a gas of hard spheres with respect to the group of space-time shifts,'' Proc. of Petrovski Seminar **8**, 218–238 (1982).
[12] M. Bauer and W. Martienssen, ''Lyapunov exponents and dimensions of chaotic neural networks,'' J. Phys. A **24**, 4557–4566 (1991).
[13] K. Kaneko, ''Towards thermodynamics of spatiotemporal chaos,'' Prog. Theor. Phys. Suppl. **99**, 263–287 (1989).
[14] N. Parekh, V. R. Kumar, and B. D. Kulkarni, ''Analysis and characterization of complex spatio-temporal patterns in nonlinear reaction-diffusion systems,'' Physica A **224**, 369–381 (1996).
[15] N. Parekh, V. R. Kumar, and B. D. Kulkarni, ''Control of spatiotemporal chaos: a study with an autocatalytic reaction-diffusion systems,'' Pramana, J. Phys. **48(1)**, 303–323 (1997).
[16] D. Ruelle, ''Five turbulent problems,'' Physica D **7**, 40–44 (1983).
[17] P. Manneville, ''Liapounov exponents for the Kuramoto-Sivashinsky model,'' in *Macroscopic modeling of turbulent flows*, Lecture Notes in Physics (Springer-Verlag, Berlin, 1985) Vol. 230, pp. 319–326.
[18] S. Ørstavik, R. Carretero-González, J. Huke, D. S. Broomhead, and J. Stark, ''Interleaving and estimation of intensive measures in spatio-temporal systems from time-series,'' (in preparation).
[19] B. R. Parlett, *The symmetric eigenvalue problem* (Prentice-Hall, Englewood Cliffs, NJ, 1980).
[20] K. Kaneko, ''Transition from torus to chaos accompanied by frequency lockings with symmetry breaking,'' Prog. Theor. Phys. **69(5)**, 1427 (1983).
[21] K. Kaneko, ''Period-doubling of kink-antikink patterns, quasiperiodicity in anti-ferro-like structures and spatial intermittency in coupled logistic lattice,'' Prog. Theor. Phys. **72(3)**, 480–486 (1984).
[22] P. M. Gade and R. E. Amritkar, ''Spatially periodic orbits in coupled map lattices,'' Phys. Rev. E **47(1)**, 143–153 (1993).
[23] Q. Zhilin, H. Gang, M. Benkun, and T. Gang, ''Spatiotemporally periodic patterns in symmetrically coupled map lattices,'' Phys. Rev. E **50(1)**, 163–170 (1994).
[24] R. Carretero-González, D. K. Arrowsmith, and F. Vivaldi, ''Mode-locking in coupled map lattices,'' Physica D **103**, 381–403 (1997).
[25] R. Kapral, R. Livi, G.-L. Oppo, and A. Politi, ''Dynamics of complex interfaces,'' Phys. Rev. E **49(3)**, 2009–2022 (1994).
[26] D. Keeler and J. D. Farmer, ''Robust space-time intermittency and $1/f$ noise,'' Physica D **23**, 413–435 (1986).
[27] C. Beck, ''Chaotic cascade model for turbulent velocity distribution,'' Phys. Rev. E **49(5)**, 3641–3652 (1994).
[28] F. H. Willeboordse and K. Kaneko, ''Pattern dynamics of a coupled map lattice for open flow,'' Physica D **86(3)**, 428–455 (1995).
[29] R. Carretero-González, ''Front propagation and mode-locking in coupled map lattices,'' Ph.D. thesis, Queen Mary and Westfield College, London, U.K., 1997. http://www.ucl.ac.uk/~ucesrca/abstracts.html
[30] V. I. Oseledec, ''A multiplicative ergodic theorem. Ljapunov characteristic numbers for dynamical systems,'' Trans. Moscow Math. Soc. **19**, 197–231 (1968).
[31] P. J. Davis, *Circulant Matrices* (Wiley, New York, 1979).
[32] R. Bellman, *Introduction to matrix analysis* (McGraw-Hill, New York, 1960).
[33] S. Isola, A. Politi, S. Ruffo, and A. Torcini, ''Lyapunov spectra of coupled map lattices,'' Phys. Lett. A **143(8)**, 365–368 (1990).
[34] S. Vannitsem and C. Nicolis, ''Error growth dynamics in spatially extended systems,'' Int. J. Bifurcation Chaos Appl. Sci. Eng. **6(12A)**, 2223–2235 (1996).
[35] N. Parekh, V. R. Kumar, and B. D. Kulkarni, ''Synchronization and control of spatiotemporal chaos using time-series data from local regions,'' Chaos **8**, 300–306 (1998).
[36] S. Barnett, *Matrices: methods and applications* (Oxford U.P., Oxford, 1990), p. 349.
[37] G. Giacomelli and A. Politi, ''Spatio-temporal chaos and localization,'' Europhys. Lett. **15(4)**, 387–392 (1991).
[38] H. Furstenberg and H. Kesten, ''Products of random matrices,'' Ann. Math. Stat. **31**, 573–469 (1960).
[39] R. A. Johnson, K. J. Palmer, and G. R. Sell, ''Ergodic properties of linear dynamical systems,'' SIAM (Soc. Ind. Appl. Math.) J. Math. Anal. **18(1)**, 1–33 (1987).
[40] M. P. Hassell, H. N. Comins, and R. M. May, ''Spatial structure and chaos in insect population dynamics,'' Nature (London) **353**, 255–258 (1991).
[41] H. N. Comins, M. P. Hassell, and R. M. May, ''The spatial dynamics of host-parasitoid systems,'' J. Anim. Ecology **61**, 735–748 (1992).
[42] H. B. Wilson and D. A. Rand, ''Reconstructing the dynamics of unobserved variables in spatially-extended systems,'' Proc. R. Soc. London, Ser. B **264**, 625–630 (1997).
[43] P. Rohani and O. Miramontes, ''Host-parasitoid metapopulations: the consequences of parasitoid aggregation on spatial dynamics and searching efficiency,'' Proc. R. Soc. London, Ser. B **260**, 335–342 (1995).